Aquatic Geochemistry
https://doi.org/10.1007/s10498-024-09427-6

ORIGINAL ARTICLE

Solute Sources and Mechanism of Boron Enrichment in the Tataleng River on the Northern Margin of the Qaidam Basin

Wenxia Li[1,2,3] · Zhanjie Qin[1,2] · Weiliang Miao[1,2] · Yulong Li[1,2,3] · Wenjing Chang[1,2,3] · Yongsheng Du[1,2] · Binkai Li[1,2] · Xiying Zhang[1,2]

Received: 29 December 2023 / Accepted: 3 April 2024

Abstract

The Tataleng River (TTR), as an important tributary of the Da Qaidam Salt Lake (DQSL) and Xiao Qaidam Salt Lake (XQSL) in the Qaidam Basin (QB), has an exceptionally high B content. However, the solute sources and the provenance of B in the TTR are still unclear, which significantly hinders a deeper understanding of the source–sink processes of the boron deposits in the QB. In this study, water samples were collected from tributaries, mainstreams, mud volcanoes, hot springs, and rainwater in the TTR area. Through hydrochemical analysis, forward modeling, and B isotope geochemistry methods, combined with the previous research results, some findings were obtained. The hydrochemical type of TTR is Ca–Mg–Cl, and the major mechanism of controlling chemical composition is rock weathering. The solute sources in the TTR are mainly from dissolution of evaporites (75.9%), atmospheric precipitation (20.8%), and a minor contribution from carbonates (3.1%) and silicates weathering (0.6%). The higher B content (0.89–4.30 mg/L, mean = 2.13 mg/L) and lower $\delta^{11}B$ value (0.79‰–4.71‰, mean = 4.17‰) of the TTR indicate that the B sources are mainly from mixture of mud volcanic waters (56.19–199.98 mg/L, mean = 113.51 mg/L, − 1.26‰–2.22‰, mean = 0.85‰) in the upper reaches, and the deep groundwater near the Indosinian granite in the lower reaches. The significant difference in boron resources between the two lakes may be due to the enrichment of B in the late Pleistocene in the DQSL, which received exceptionally rich soluble B carried by the ancient TTR during an active tectonic period, while the weakening of tectonic activity and the diversion of the ancient TTR resulted in the supply of B with significantly reduced content to the XQSL. These results are helpful for a deeper understanding of the ore-forming mechanisms of the boron deposits in salt lake.

Keywords Boron · Solute sources · Salt lake · Tataleng River · Qaidam Basin

✉ Binkai Li
libk@isl.ac.cn

[1] Key Laboratory of Green and High-End Utilization of Salt Lake Resources, Qinghai Institute of Salt Lakes, Chinese Academy of Sciences, Xining 810008, China

[2] Qinghai Provincial Key Laboratory of Geology and Environment of Salt Lakes, Xining 810008, China

[3] University of Chinese Academy of Sciences, Beijing 100049, China

1 Introduction

Boron is a quintessential crustal element that is widespread in volcanic, plutonic, sedimentary, and metamorphic environments (Grew 2015), and is widely used in ceramics, detergents, fertilizers, and glass field (Ali et al. 2020; Dymova et al. 2020). Boron deposits are mainly classified into volcanic sedimentary type, sedimentary metamorphic type, silicate type, and modern salt lake type. The types of boron deposits discovered in China are mainly sedimentary metamorphic type and modern salt lake type, with their resource reserves accounting for 38.1% and 52.4% of the national reserves, respectively (Lin et al. 2017). Among them, the modern salt lake-type boron deposits are mainly distributed in the Qinghai–Tibet Plateau (QTP) region of China, and the solid boron deposits (6.39 million tons, calculated as B_2O_3) and liquid boron deposits (0.64 million tons, calculated as B_2O_3) in salt lakes such as DQSL and XQSL account for about 60% of the explored salt lake-type boron resources in China (Wei 2002), thus having significant economic and research value.

Systematic research has been conducted on the formation mechanism of boron resources in the DQSL (with a total boron resource of approximately 6.23 million tons, B_2O_3) (Yang 1983; Zhang 1987). It is believed that bedrock weathering (including tourmaline granite), deep boron-rich groundwater replenishment, and dissolution of salt aeolian deposits may be important sources for boron deposits in the DQSL (Stober et al. 2016; Jiang et al. 2021; Li 2022). Kong et al. (2021) further constrained the contribution ratios of different boron sources by using radium isotopes to trace various waters around the DQSL. They found that deep hot groundwater contributed 60.1% of the B in the DQSL. However, due to the small flow rate of hot springs, the lack of research on the enrichment and mineralization processes of hot spring fluids in surface environments, and considering that the formation age (Early Holocene, 8620 years ago) of boron resources in the DQSL (Gao et al. 2019), the view that deep hot springs are the main source of boron materials based on the understanding of the modern surface water in the Da Qaidam Basin is obviously debatable, and the role of other sources in the lake evolution process must also be considered (Xiao et al. 1994).

The DQSL and XQSL were once a unified basin before approximately 30,000 years ago; however, under the intensifying arid climate conditions, they evolved into two separate basins (Zheng et al. 1989). The TTR, which currently supplies water to the XQSL, used to be the main source for the DQSL before the Upper Pleistocene (Yang 1983). The upstream of the TTR is characterized by numerous mud volcanoes, some of which still overflow with boron-rich water (Zhang 2015). Additionally, the upper of Tataleng River contains sedimentary boron deposits such as the Juhongtu ancient hot spring deposit and several other sedimentary boron mineralization points like Wulanbaomu and Kaotiaozhaohuo (Zheng et al. 1989). Furthermore, the average B content in rocks within the TTR basin is more than 10 times higher than the normal rock Clark value (Yang 1983). These findings indicate the significant role of the TTR in the formation of boron resources in the DQSL and XQSL. However, despite the significantly higher B concentration in TTR (1.37 mg/L) compared to major rivers worldwide (0.01 mg/L) (Gaillardet et al. 2014), the lack of comprehensive basin-scale studies hampers our understanding of boron sources and transport processes in this region, which, in turn, constrains our comprehension of boron deposit formation mechanisms in the DQSL and XQSL.

In arid regions, the accurate identification of the recharge end-members of brine resources in salt lakes is essential for understanding the origin of brine deposits. The identification and quantification of sources based on the water chemical composition and isotope

tracing are typical methods currently used in the study of the origin of resource elements in salt lakes. Satisfactory results have been achieved in the Guayatayoc Salt Lake in the South American Puna Plateau (López Steinmebtz 2017), as well as in the QB, Eastern and Western Taijinar Salt Lakes, and DQSL on the QTP (Li et al. 2021; Kong et al. 2021; Zhang et al. 2022; Miao et al. 2022). The water chemical composition of a watershed records important information about the typical solutes provided by various input sources and their proportional relationships. Many studies have used forward or reverse models to calculate the relative contribution rates of different sources (atmospheric precipitation, rock weathering, etc.) to solutes in river water (Wu et al. 2008; Noh et al. 2009; Zheng et al. 2023). This information is crucial for quantitatively studying the main sources in the watershed, rock weathering characteristics, and even estimating CO_2 consumption during weathering processes (Gibbs 1970; Gaillardet et al. 1999; Wu et al. 2005; Moon et al. 2007; Wu 2016; Han et al. 2021).

Additionally, B, as a highly incompatible lithophile element, plays a unique tracing role in geological processes such as hydrothermal alteration (Jiang 2001, Jiang et al. 2004, 2008), water–rock interactions (Barth 1998; Pennisi et al. 2000), and surface weathering (Rose et al. 2000; Muttik et al. 2011). It is commonly used to identify element sources (Sun et al. 1989; Xiao et al. 1992, 2001; Vengosh et al. 1991, 1998) and analyze lake evolution processes (Liu et al. 2000; Foster 2008). B has two stable isotopes, and due to the large mass difference, the spatial configuration of borate ions, which determines the distribution characteristics of isotopes in solution, is controlled by pH value and B concentration (heavy isotope ^{11}B is enriched in $B(OH)_3$, while light isotope ^{10}B is enriched in $B(OH)_4^-$, Kakihana et al. 1977). Therefore, many geological processes, including evaporation, ion exchange, and adsorption, may cause significant B isotope fractionation ($-70‰$ to $+75‰$) (Williams and Hervig 2004), making B isotopes highly potential for tracing provenance and different geological processes. Recently, significant progress has been made in using B isotopes to trace the provenance of B in salt lakes (Xiao et al. 1992, 1999; Vengosh et al. 1995; Xiao et al. 2013; Lü et al. 2014; Han et al. 2021).

In this study, we conducted detailed fieldwork and sampling in the DQSL and XQSL areas within the DaChaidan region, focusing on various water bodies such as rivers, salt lakes, hot springs, rainfall, and particularly the mud volcano waters in the upper reaches of the TTR. We present comprehensive results on the hydrochemistry of these waters, including major and trace elements. By incorporating B isotope analysis and forward model calculations based on hydrochemical composition, we aim to provide new insights into the origin and enrichment mechanisms of boron in the DQSL and XQSL. Additionally, we seek to quantitatively assess the solute sources and controlling factors in the TTR. The findings of our study are anticipated to enhance understanding of the genetic mechanisms of boron-rich salt lakes.

2 Geological Setting

The QB is a typical inland arid basin with a total area of 12×10^4 km^2 and an elevation ranging from 2600 to 3000 m. The Qilian Mountains are located in the northeast of the basin, trending NW–SE. The southern side of the mountains, including Zongwulong Mountain, Dakendaban Mountain, Xitie Mountain, and Lvliang Mountain, forms the central and northern margin of the basin, with elevations ranging from 3500 to 5656 m. The Altun Mountains are located in the western part of the basin, with elevations ranging

from 3000 to 5000 m. The Kunlun Mountains are located in the southern margin of the basin, with elevations of approximately 3500–5500 m (Zhang 1987) (Fig. 1a). The Qilian orogenic belt between the Alxa Block and the Qaidam Block can be divided into the North Qilian Belt, the Central Qilian Belt, the South Qilian Belt, the Quanji Block (Olongbuluke), and the North Qaidam Ultra-High-Pressure Metamorphic Belt (Song et al. 2013) (Fig. 1a). In the northern margin of the QB, strata from the Proterozoic to the Quaternary are exposed intermittently. Among them, the Dakendaban Formation developed in the Lower Proterozoic, the Changcheng Series and Jixian Series developed in the Middle Proterozoic, the Tanjianshan group developed in the Late Ordovician, the Maoniushan Formation developed in the Late Devonian, and the Amunike Formation, Chuanshangou Formation, Chengqianggou Formation, and Huaitoutala Formation developed in the Carboniferous. The Jurassic to Early Cretaceous is characterized by the Xiaomeigou Formation, Huoshaoshan Formation, Yinmagou Formation, and Dameigou Formation. Since the Cenozoic, the Lulehe Formation, Xiaganchaigou Formation, Shangganchaigou Formation, Youshanshan Formation, Shizigou Formation, and Qigequan Formation have developed (Cai et al. 2019).

The DQSL, located in the mountain basin of the North Qaidam Ultra-High-Pressure Metamorphic Belt, was originally a unified basin. However, during the late Pleistocene, the new tectonic movement caused the middle section between the two lakes to rise, forming two independent closed inland basins (Yang 1983). The basin margins are characterized by small areas of Cretaceous, Jurassic, and Tertiary deposits, while Quaternary deposits are distributed from the foothills to the lake basin, including alluvial fans, fluvial deposits, and lacustrine deposits (Yang 1983; Zheng et al. 1989). Various magmatic rocks from different periods are exposed in the area, with the distribution of Mesozoic pegmatite granite being

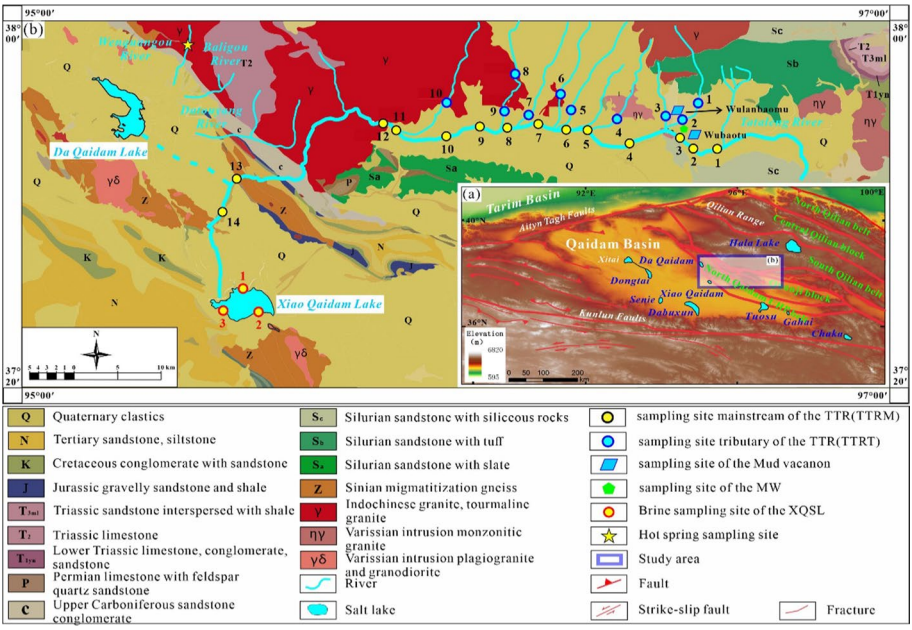

Fig. 1 Maps of the geological structure and sampling locations in the study area. **a** Schematic diagram of the regional geological structure in the QB (modified from Zhang 1987) and **b** geological setting and sampling locations in the TTR Basin (modified from QGMB 1960). MW (Meteoric water)

the most extensive. Granite from different periods is widely distributed in the Dakendaban Mountains, mainly including Indosinian pegmatite granite and Hercynian intrusive granite (QGMB 1960). At the same time, the region is characterized by the development of fault structures, with a thrust fault starting from the north of Yuqia and extending southeast through Da Qaidam, Baligou, Datouyanggou, TTR, and Lvcaoshan, roughly along the southern edge of the Dakendaban Mountains, and terminating east of Erwenwulan (Pang et al. 2015).

The lakes of DQSL and XQSL are supplied by a total of 12 rivers, with the main river being the TTR. This river originates from the Kuerleike Mountains and the southern mountains of Hala Lake, with a catchment area of 4771 km^2 and a total length of 210 km. The average annual flow is 3.68 m^3/s, with an annual runoff of 1.2×10^8 m^3 (Zhang 2005). Currently, the TTR supplies water to XQSL on the surface and to DQSL in the form of underground flow (Dang 2020). The Datouyang River originates from the Kuerleike Mountains, formed by the convergence of meltwater from ice and snow, as well as groundwater from bedrock fractures. It has a total length of 230 km and a flow rate of 0.8–1.0 m^3/s. The Baligou River has a short distance and infiltrates underground at a distance of 1.0-km northeast of DQSL. It emerges as a spring after passing through the town of Da Qaidam and flows into the lake. Wenquangou has multiple bead-like hot springs, which converge into a river and supply water to DQSL. The bedrock outcrops at the springs are granite. The hot springs emerge from a major WNW–ESE-trending fault system between Qaidam granite and Paleozoic sediments. The group of springs occurs in narrow area along the fault. The setting of the springs suggests that the permeability of the granitic bedrock in the outer fault zone (damage zone) is enhanced at the localities where the springs ascend, and it is strongly reduced down-slope of the discharge points (fault core) (Stober et al. 2016). According to statistics, there are a total of 87 hot springs, with an average water temperature of 60–70 °C, mainly overflowing along tectonic fractures and fractured zones in the granite gneiss north of Da Qaidam town (Wang et al. 1998). Currently, XQSL is supplied by the perennial TTR, and in the middle reaches of the TTR, there are several small active mud volcanoes (Wulanbaomu, Wubaotu, etc.), mainly emitting jets and carrying some muddy and boron-rich water (Zhang 2015).

3 Materials and Methods

3.1 Sampling Processing

In June 2023, a total of 37 water samples were collected for analysis. They included 24 samples from the TTR (10 tributary samples (TTRT) and 14 mainstream samples (TTRM)), five samples from the hot spring of the DQSL (HS), three samples from the XQSL, four mud volcanic water samples (MVW), and one sample of meteoric water (MW) (Fig. 1b). Each brine sample was stored in two 500-mL polyethylene bottles. Prior to sampling, all containers were soaked in 10% nitric acid for 48 h, cleaned with deionized water, and dried in an oven. The containers were then moistened with sample water and filled up. To maintain the ionic state of the chemical components and prevent precipitation and adsorption, pure nitric acid (68%) was added to the samples, and the containers were sealed for transportation. A 0.45-μm cellulose acetate filter membrane was used to filter the samples immediately in the laboratory for cation testing.

3.2 Chemical Composition

The concentrations of major and trace cations (K^+, Na^+, Ca^{2+}, Mg^{2+}, SO_4^{2-}, and B^{3+}) in all water samples were measured using an inductively coupled plasma optical emission spectrometer (ICP-OES, ICAP6500 DUO, Thermo Fisher Scientific). The CO_3^{2-} and HCO_3^- concentrations were immediately determined by potentiometric titration. The concentrations of Cl^- were measured using $Hg(NO_3)_2$ potentiometric titration. Each reported value represents the mean of two different measurements, and the analytical precision for major cations and anions was better than ± 2%. The entire analysis was conducted at the Qinghai Institute of Salt Lakes, Chinese Academy of Sciences, following the procedures of the institute by the methods for water chemical analysis (ISLCAS 1988). Data on water samples are initially checked for quality using normalized inorganic charge balance (NICB) ratio ($TZ^+ = Na^+ + 2Ca^{2+} + 2Mg^{2+} + K^+$, $TZ^- = HCO_3^- + Cl^- + 2SO_4^{2-} + NO_3^- + F^-$, $NICB = (TZ^+ - TZ^-)/TZ^+ \times 100\%$). The NICB of various samples is within ± 9% (mean value − 3.43%), indicating that the chemical composition testing is ideal (Table S-1).

3.3 Boron Isotope

The chemical purification steps for sample B include the following: Firstly, the sample solution is adjusted to weak alkaline conditions (pH 7–8) and then injected into an exchange column containing Amberlite IRA 743 boron-specific resin. The resin is washed with 10 mL of high-purity water and eluted with 10 mL of 75 °C 0.1 M HCl. The eluate is collected and placed in a drying oven (60 °C) to concentrate to approximately 0.5 mL. Thirdly, the concentrated sample solution is injected into a mixed resin column containing equal volumes of strong acidic cation resin (Dowex 50Wx8, 200–400 mesh) and weak alkaline anion resin (Ion-exchange II, 60–100 mesh) to remove residual HCl. The column is then washed with boron-free high-purity water, and the eluate is collected. Finally, the eluate is mixed with equimolar amounts of mannitol and Cs_2CO_3, and the mixture is further concentrated and evaporated to 0.3 mL at 60 °C. The isotopic values of B in sample are analyzed using a mass spectrometer (Fan et al. 2015; Wei et al. 2014), installed at the Salt Lake Chemical Analyzing and Testing Center, Qinghai Institute of Salt Lakes. All water used in the experiment is deionized water that has undergone two rounds of sub-boiling distillation and boron-specific resin exchange to obtain low-boron water. To avoid boron contamination, the experiment is conducted using polytetrafluoroethylene, polyethylene, or quartz vessels.

The determination of B isotope composition was performed on Triton (Thermo Fisher Scientific) P-TIMS using the $CsBO^{2+}$-graphite double coating method (Xiao et al. 1988). Briefly, 2 μL of graphite suspension and 1 μL of the sample solution were separately coated on a degassed Ta strip and dried for 5 min under 1.2 A conditions. The ion intensities of mass numbers 308 ($^{133}Cs_2{}^{10}B^{16}O^{2+}$) and 309 ($^{133}Cs_2{}^{10}B^{16}O^{2+}$) were obtained using a custom-made 308 and 309 Faraday cup system. The ratio of ^{11}B to ^{10}B was determined after oxygen isotope correction. The B isotope composition $\delta^{11}B$ is expressed as follows:

$$\delta^{11}B(‰) = \left[\left({}^{11}B/{}^{10}B \right)_{\text{sample}} \Big/ \left({}^{11}B/{}^{10}B \right)_{\text{standard}} - 1 \right] \times 1000$$

The standard material is NIST 951, having average internal analytical precision and the external reproducibility of 0.35‰ (2 SE) and 0.04‰ (2σ), respectively. $^{11}B/^{10}B_{\text{Standard}}$

NIST 951 was 4.05537 ($n=4$), the certified value by NIST. The test work was conducted in the Qinghai Institute of Salt Lakes, Chinese Academy of Sciences.

3.4 Forward Model

The forward model has been used to calculate the relative contribution rates of different solute sources (atmospheric precipitation, rock weathering, etc.) in river water (Wu et al. 2008; Noh et al. 2009; Zheng et al. 2023). The model assumes that the chemical composition of dissolved loads in the river is the result of mixing from different sources, including atmospheric input, silicate and carbonate weathering, and evaporite dissolution (Galy and France-La-nord 1999; Moon et al. 2007; Wu et al. 2008). Na mainly comes from silicate and salt rocks, with only a small fraction from carbonate and atmospheric sources, while Ca, Mg, and K primarily come from the dissolution of these three types of rocks. Cl mainly comes from atmospheric input and the dissolution of salt rocks, so in the dissolved load, $Cl_{riv}=Cl_{rw}+Cl_{eva}$. The mass balance equation for any element Z is $Z_{riv}=Z_{rw}+Z_{car}+Z_{sil}+Z_{eva}$, where riv, rw, car, sil, and eva represent river water, rainwater, carbonates, silicates, and evaporates, respectively.

4 Results

4.1 Hydrochemical Characteristics of Different Waters

The pH of samples of TTR, HS, XQSL, MVW, and rainwater (6.7–8.9) indicates weak acidity and alkalinity, similar to the Golmud River (GR), Nalenggele River (NR), and Hongshui River (HR) in the southern Kunlun Mountains of the basin (Table S-1 and references therein). The total dissolved solids (TDS) range of the TTR tributaries is 0.38–0.65 g/L, with an average of 0.52 g/L, and the main stream TDS range is 0.63–1.33 g/L, with an average of 0.92 g/L. The TDS range of HS is 1.07–1.19 g/L, with an average of 1.10 g/L, and the average TDS of XQSL brine and rainwater are 37.48 g/L and 0.01 g/L, respectively. The TDS of MVW is from 3.41 to 6.05 g/L, with average value of 4.67 g/L. Comparing with the GR (0.63 g/L, $n=5$), NR (0.88 g/L, $n=14$), and HR (1.66 g/L, $n=3$) in the southern basin (Li et al. 2021; Miao et al. 2022; Zhang et al. 2022; Zhu et al.1990), it can be found that the TDS of river water in the basin is generally similar, while the HR, which is replenished by hot springs, is significantly higher than other rivers.

The tributaries of the TTR are significantly rich in Ca, accounting for 40–60% of the total composition. The next most abundant elements are Na + K, comprising approximately 30%, while Mg has the proportion between 10 and 17%. In the main stream of the TTR, the proportion of Ca decreases to about 30–40%, which is similar to the proportion of Na + K, while the proportion of Mg remains relatively stable. The cation characteristics of the TTR main stream are similar to those of the GR but distinct from the NR and the HR. The DQSL and XQSL are significantly rich in Na + K, primarily controlled by evaporation, while the Ca content in rainwater is relatively high at about 80%. The hot spring samples are predominantly composed of Na + K, accounting for approximately 80–90%. The cations of MVW are similar to that of the main stream of TTR (Fig. 2).

In terms of anions, the most significant characteristic is the lowest proportion of SO_4 content in all samples. Most of the samples from the TTR tributary are similar to the main stream samples, dominated by Cl, accounting for about 60–80%. There is

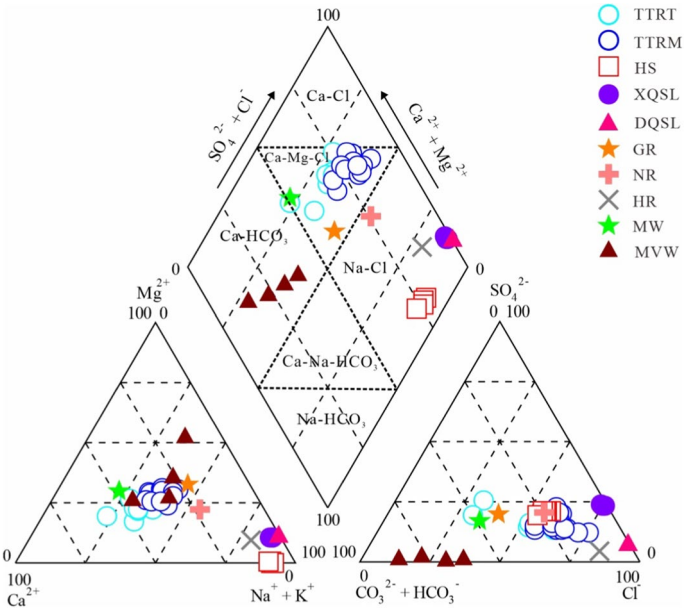

Fig. 2 Piper diagram of hydrochemical composition of different waters in the study area (Modified from (Piper 1944). TTRT (tributary of the TTR), TTRM (mainstream of the TTR), HS (hot spring), XQSL (Xiao Qaidam Salt Lake), DQSL (Da Qaidam Salt Lake), GR (Golmud River), NR (Nalenggele River), HR (Hongshui River), WM (Meteoric water), and MVW (Mud volcanic water)) (Table S-1 and references therein)

a gradual increase in Cl content from upstream to downstream, while HCO_3 gradually decreases. Due to evaporation, the brines of the DQSL and XQSL are predominantly chloride, indicating that it has evolved to the chloride stage. The HS are also dominated by Cl, accounting for about 80%, similar to the NR and the HR influenced by the hot springs. Rainwater is mainly composed of HCO_3, combined with Ca as the dominant cation, indicating a possibility of dissolution of carbonate mineral particles. The MVW is clearly rich in HCO_3 and contains virtually no SO_4, indicating that the release of CO_2 gas during its slow eruption process may be the main reason. According to the Piper diagram, it can be seen that both the HS and the brine of XQSL are Na-Cl type, rainwater is Ca-HCO_3 type, and the TTR is Ca–Mg–Cl type (Fig. 2).

The average B content in the tributaries and main stream of the TTR is 0.82 mg/L ($n=10$) and 1.76 mg/L ($n=14$), respectively. Rainwater has a B content of 0.01 mg/L, while the XQSL brine and HS have B contents of 93.31 mg/L ($n=3$) and 47.31 mg/L ($n=5$), respectively. The B content range in MVM is 56.19–199.98 mg/L, with a mean of 113.51 mg/L ($n=4$). This indicates that the B content in surface runoff is generally one order of magnitude lower than that in salt lake brines and hydrothermal waters. Compared to other rivers in the Qilian Mountains, such as Bayin River (0.33 mg/L, $n=4$), Yuqia River (0.52 mg/L), Haerteng River (0.27 mg/L), Alar River in the Altun Mountains (0.35 mg/L, $n=3$), and the GR (0.43 mg/L, $n=3$) and HR (1.90 mg/L) in the Kunlun Mountains (Jiang et al. 2021; Zhang et al. 2022), it is found that the B content in the main stream of the TTR is similar to that in the NR and HR, but significantly higher than other rivers in the basin. Furthermore, the B content in the main stream of the TTR

is one to two orders of magnitude higher than that in the Amazon River (0.01 mg/L), Yangtze River (0.01 mg/L), Yellow River (0.15 mg/L), and the global average for rivers (0.01 mg/L) (Gaillardet et al. 2014; Qu et al. 2019), indicating its anomalous enrichment of B content.

4.2 B Isotopic Compositions

The $\delta^{11}B$ values of the tributaries of the TTR show a wide range of variation, from −4.75 to 19.87‰ (mean = 4.53‰, $n = 6$). In contrast, the $\delta^{11}B$ values of the main stream decrease gradually from 16.82‰ in the upstream to 0.79‰ in the downstream, with a mean of 7.41‰ ($n = 11$). The $\delta^{11}B$ values of the HS (1.34‰, $n = 2$) and the brine of the XQSL (1.72‰, $n = 3$) are significantly lower than those of the tributaries and main stream of the TTR in the upstream samples, but similar to those in the downstream. The $\delta^{11}B$ values of mud volcano water range from −1.26 to 2.22‰, with a mean value of 0.85‰ ($n = 3$).

5 Discussion

5.1 Sources of Solute

5.1.1 Atmospheric Inputs

The main sources of solutes in river water include atmospheric input, rock weathering, and deep water (Gaillardet et al. 1999; Wu 2016). TTR is located far away from densely populated areas, so it is minimally affected by human activities and can be disregarded.

The main sources of atmospheric input are dust and sea salt. However, since the study area is located inland and far from the ocean, the influence of sea salt input is minimal. In contrast, the Golmud, which is located 200-km southwest of the study area, is a typical inland arid region where frequent dust storms occur in spring and autumn, providing a significant amount of dust to the atmosphere (Zhu et al. 2008). Recent studies have shown that the dust storms in the QB are primarily composed of soluble salt minerals such as rock salt, gypsum, and anhydrite (Geng et al. 2021; Zhang et al. 2020). Therefore, the wind erosion process is likely to contribute salt-containing substances to the atmosphere. In recent years, researchers have studied the origin of hot springs in the northern part of Da Qaidam and suggested that the high Cl/Br ratio may be closely related to the dissolution of windblown sediments (rock salt, gypsum, or borate minerals) from the Qilian Mountains region (Stober et al. 2016). All of these findings indicate that atmospheric dust deposition makes a certain contribution to the solute content in rivers.

5.1.2 Rock Weathering

The Gibbs diagram is an effective analytical method for qualitatively assessing the hydrochemical impacts of regional processes such as evaporation-concentration, rock weathering leaching, and atmospheric precipitation on surface water (Gibbs 1970). In Fig. 3, the tributaries and mainstreams of the TTR are primarily influenced by rock weathering and present a extend trend to evaporation precipitation (Gibbs 1970). This is similar to the ion sources of the Heihe River, Shule River, and Buha River in the Qilian Mountains under the same

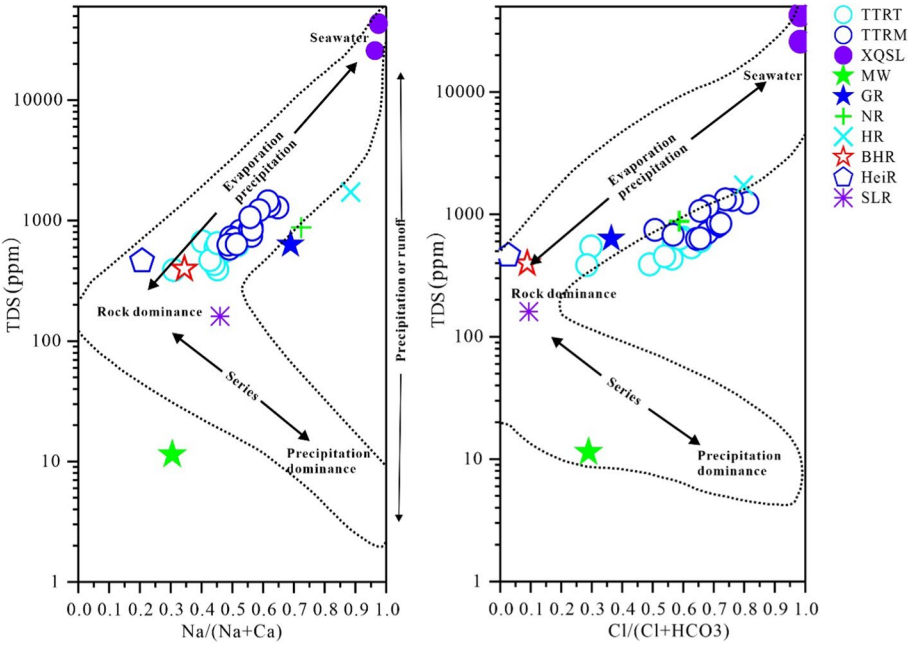

Fig. 3 Gibbs diagram of different waters in the study area (modified from Gibbs 1970). TTRT (tributary of the TTR), TTRM (mainstream of the TTR), HS (hot spring), XQSL (Xiao Qaidam Salt Lake), GR (Golmud River), NR (Nalenggele River), HR (Hongshui River), WM (Meteoric water), BHR (Buha River), HeiR (Hei River), and SLR (Shule river) (Table S-1)

climatic background (Qu et al. 2019). The XQSL brine is clearly controlled by evaporation, which is consistent with its high TDS.

The [Na]/[Cl] molar ratio is an important indicator of rock salt dissolution in water bodies. In Fig. 4a, the [Na]/[Cl] ratio of atmospheric precipitation is below the line of rock salt dissolution, indicating the presence of other chloride salt minerals in addition to halite in the dust fall. Except for sample TTRT-1, all other samples from tributaries and the main stream are below the line of rock salt dissolution. With the increase in TDS in the water, there is little overall change in the [Na]/[Cl] ratio, indicating a similar and stable source of Na and Cl in the TTR. The dissolution of rock salt in strata or on the surface is the primary sources.

The Na content of TTRM-3 increased slightly when it passed through the Wulanbaomu and Wubaotu mud volcanoes, while the Na content of TTRM-13 and TTRM-14 samples decreased when they passed through the Indosinian granite. The salt crusts around Wulanbaomu and Wubaotu mud volcanoes mainly consist of calcite, gypsum, halite, and ulexite (Zhang 2014). After hydrochemical simulation, the mineral composition of the MVW includes halite, ulexite, a small amount of mirabilite, and a large amount of carbonate (Zhang 2015). Based on this, it can be inferred that the TTRM-3 sample may be influenced by the dissolution of borate minerals (such as ulexite and borax) in the surrounding formations of the mud volcano or the mixing of sodium-enriched MVW (Zhang 2015). On the other hand, the TTRM-13 and TTRM-14 samples may be diluted by groundwater or fracture water in the tectonic zone of canyon of the TTR (Fig. 1). The TTRT-1 is close to the

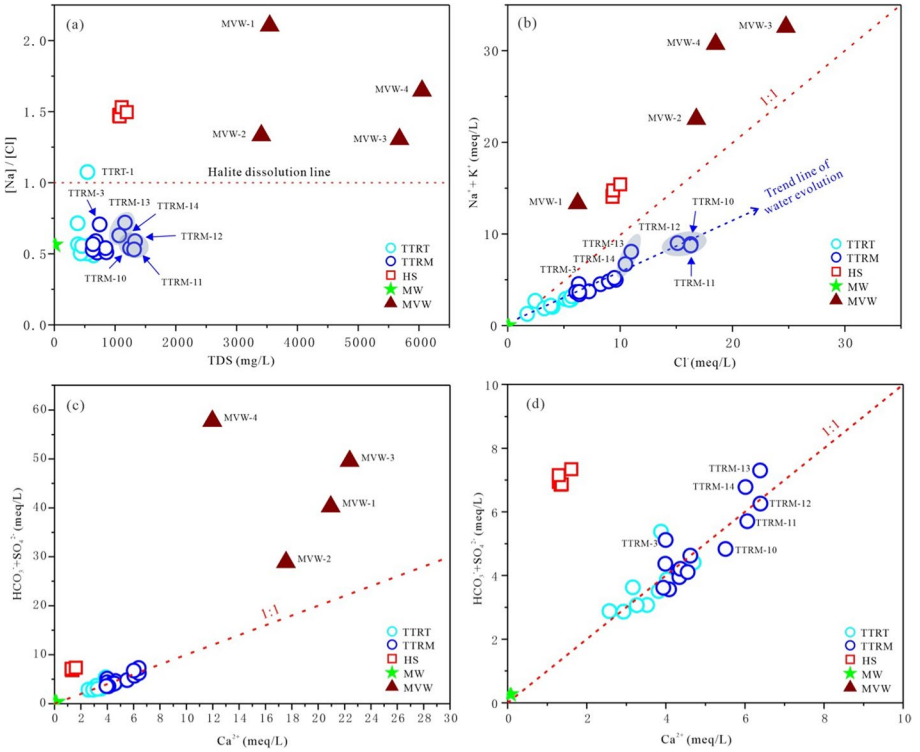

Fig. 4 Ionic relationships in different waters in the study area. There is strongly positive correlation between (Ca) and ($HCO_3 + SO_4$) which also clusters to 1:1 line, indicating that evaporite is an important source of the dissolved loads in rivers. TTRT (tributary of the TTR), TTRM (mainstream of the TTR), HS (hot spring), WM (Meteoric water), and MVW (Mud volcanic water)

rock salt dissolution line, indicating that the strata it passes through are rich in rock salt or other Na-containing minerals.

In Fig. 4b, the overall evolution trend of Na + K and Cl in the TTR is consistent. This is mainly attributed to the dissolution of soluble salt minerals containing Na and K present in the regional Quaternary strata or atmospheric dust deposition. The molar ratio of Na + K to Cl further indicates that the dissolution of rock salt cannot provide all the Cl for the TTR. The high levels of Cl in river water, apart from being attributed to the dissolution of evaporite minerals, may also be associated with the consumption of Na in strata, such as the precipitation of Na_2CO_3 and $NaHCO_3$ minerals in formations near the mud volcanoes upstream of the TTR (Zhang 2014). This phenomenon is similar to the low Na–Cl ratios observed in the Godavari and Mahanadi Rivers in India (Chhabra 1996). In Fig. 4c and d, there is a good correlation between the molar ratio of $HCO_3 + SO_4$ to Ca (1:1) in samples of the TTR. This suggests that the dissolution of carbonate minerals (calcite or aragonite) and sulfate minerals (gypsum) may be the main sources of Ca in the TTR. This is consistent with the presence of a certain amount of carbonate minerals in the Upper Quaternary strata of the upstream TTR (China Geological Survey 2004). Therefore, the major ions of the hydrochemical composition of TTR are mainly controlled by the dissolution of evaporite (halite and sulfate) and carbonate minerals.

5.2 Quantification of Input Sources

5.2.1 Atmospheric Input

Cl is an important indicator for assessing atmospheric input, but its concentration in rocks is very low (Moon et al. 2007). The previous studies have typically assumed that rainwater has the lowest Cl content in the water system to correct for the composition of water inputs. However, rivers on the QTP are influenced by high-altitude and arid climates, and evaporite rocks are widely distributed. As a result, the Cl and Na content of dissolved salt rocks in river water is higher, with lower elemental content only near glaciers and snow lines. Simply using the minimum Cl concentration in river water for correction may introduce significant uncertainties (Wu et al. 2008, Wu 2016; Zhao et al. 2007). Therefore, the study evaluates the impact of atmospheric input on river water Cl by considering the product of rainwater Cl concentration and concentration factor within the watershed.

Based on the analysis of the Qilian Mountain glaciers, snowfall, rainfall, and the samples collected in the study, the average Cl content in the glaciers and precipitation in the Qilian Mountain region was 0.041 mmol/L (Table S-2). This is similar to the average Cl content in rainfall (snow) in the QTP region (0.049 mmol/L) (Zhao et al. 2007). In the Da Qaidam region, the evaporation rate is much higher than the rainfall, and the evaporation of rivers can cause the concentration of elements in the water. The concentration factor can be estimated using the formula $F = W_{sw}/W_{riv}$ (where W_{sw} is the rainfall amount, and W_{riv} is the river runoff). In this study, the rainfall and runoff data for June from 2018 to 2022 in the study area were collected, and the river F value in the study area was found to be 2.52 (Table S-2, references and calculation method therein), which falls within the concentration factor range of rivers in the QTP region (1.4–5.6) (Zhao et al. 2007). Therefore, the critical value of Cl content in rainfall in the study area is estimated to be 0.103 mmol/L.

If the Cl content in the river water is below a critical value, the Na contribution from rainwater in the river water is given by: $X(Na)_{rw} = (Cl/Na)_{riv}/(Cl/Na)_{rw} \times 100\%$. If the Cl content in the river water exceeds the critical value, the Cl contribution ratio from rainwater is given by: $X(Cl)_{rw} = Cl_{crit}/Cl_{riv} \times 100\%$. In this case, the Na contribution in rainwater is given by: $X(Na)_{rw} = (Cl/Na)_{riv} \times X(Cl)_{rw}/(Cl/Na)_{rw} \times 100\%$, where Cl_{crit} is the critical Cl content. The ratios of other elements in rainwater can be calculated similarly. We found that the average contribution rates of solutes from rainfall to the TTR tributary and the main stream are 25.1% ($n = 10$) and 16.6% ($n = 14$), respectively (Table S-3 and Fig. 5), indicating that atmospheric input has a certain influence on the chemical composition of rivers in this region, which is consistent with the research findings on the contribution of rainfall to river water in the inland rivers of the QTP (Wu 2016).

5.2.2 Evaporites Dissolution

Assuming that all residual Cl in the river water after rainfall correction comes from halite ($Cl_e = Cl_{riv} - Cl_{rw}$, $Na_e = Cl_e$), and all SO_4 comes from gypsum or anhydrite ($SO_{4e} = SO_{4riv} - SO_{4rw}$, $Ca_e = SO_{4e}$), the contribution of halite and sulfate dissolution to cations in the river water can be expressed as follows: Total cations can be calculated as follows: $TZ^+ = 2Ca_{riv} + 2Mg_{riv} + Na_{riv} + K_{riv}$; $Halite\% = Cl_e/TZ^+$, $Gypsum/Anhydrite\% = SO_{4e}/TZ^+$, $\sum Cation_{eva} = Halite\% + (Gypsum/Anhydrite)\%$. The average contribution of halite to solutes in the main stream and tributaries of the TTR is 57.1% ($n = 10$) and 69.1% ($n = 14$),

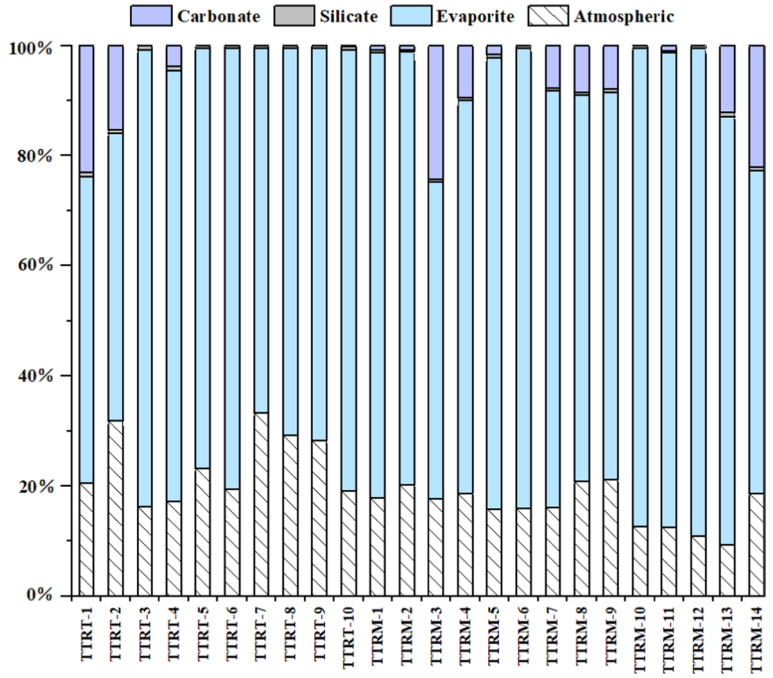

Fig. 5 Solute contribution of precipitation, evaporites, silicates, and carbonates to tributaries and mainstreams of the TTR

respectively, while the average contribution of sulfate is 17.7% ($n=10$) and 7.9% ($n=14$) for the main stream and tributaries, respectively. Therefore, the contribution of evaporite to the TTR main stream and tributaries is 74.9% and 77.0%, respectively (Table S-3 and Fig. 5). The high contribution of salt rock dissolution to solutes in the TTR is consistent with the weathering characteristics of inland rivers in the QTP (Wu 2016).

5.2.3 Silicate and Carbonate Weathering

Assuming that all remaining Na after rainfall and rock salt correction is derived from silicates, and all remaining K after rainfall correction is derived from silicates, the silicate components of Na_{sil} and K_{sil} can be estimated as follows: $Na_{sil}=Na_{riv}-Na_{rw}-Na_{eva}$, $K_{sil}=K_{riv}-K_{rw}$. Assuming that Ca and Mg are released into the river water from silicates in a fixed ratio relative to Na, it can be expressed as follows: $Ca_{sil}=Na_{sil}\times(Ca/Na)_{sil}$, $Mg_{sil}=Na_{sil}\times(Mg/Na)_{sil}$. Since the range of Ca/Na and Mg/Na ratios from silicate weathering in this region is 0.2–0.5 and 0.12–0.36, respectively (Wu 2016), this study adopts the general values of $(Ca/Na)_{sil}=0.35$ and $(Mg/Na)_{sil}=0.24$ (Gaillardet et al. 1999) for silicate weathering in different global basins. The total cations from silicate weathering can be calculated as follows: $TZ_{sil}=2Ca_{sil}+2Mg_{sil}+Na_{sil}+K_{sil}$. Therefore, the proportion of total cations contributed by silicates in the river water is: $(\sum Cat)_{sil}=TZ^{+}{}_{sil}/TZ^{+}$.

The calculations are based on the following two assumptions. Firstly, allocating all sulfate to gypsum/anhydrite instead of $NaSO_4$ would result in an overestimation of Na_{sil} and consequently an overestimation of silicate weathering. Secondly, negative values were

obtained when calculating Na_{sil}, which may be due to the neglect of the contribution of Cl ions that are not related to Na. However, it was found from the hydrochemical characteristics that silicate weathering in the basin is relatively weak, so these negative values were treated as having no contribution in this study. The results show that the average contribution rate of silicate weathering to the solute in the tributaries of the TTR is 0.6% ($n=10$), and the contribution rate to the main stream is 0.5% ($n=14$). After correcting for rainfall, evaporite, and silicate, the remaining cations can be attributed to carbonate weathering. The results show that the average contribution of carbonate weathering to the solute of the tributaries of the TTR is 4.2% ($n=10$), while the average contribution to the main stream is 6.1% ($n=14$) (Table S-3 and Fig. 5).

In summary, it can be concluded that the solute in the TTR mainly originates from the dissolution of evaporite in the strata or on the surface, followed by atmospheric precipitation. Due to the widespread presence of Quaternary formations in the region, the dissolution of carbonate is also essential, while the low rate of silicate weathering, caused by the dry and cold climate conditions in the study area, contributes the least to the river solute. The average ratio of $Cl+SO_4$:HCO_3+CO_3: Si for the entire basin in the study area is 172:53:1 (Table S-1), which also confirms this point.

5.3 Provenance of B in the TTR

The sources and formation mechanisms of major and trace ions in waters are not entirely consistent. To further understand the anomalous enrichment mechanisms of B in the TTR, we conducted a study on the provenance of B. The sources of element B in rivers generally include anthropogenic factors, atmospheric input, rock weathering (evaporite, carbonate, and silicate rocks), and deep water mixing (Mao et al. 2019). As mentioned earlier, there is minimal human activity in the study area, with almost no industrial or agricultural production activities. Therefore, the impact of anthropogenic activities on the B content in rivers can be disregarded.

Atmospheric inputs typically include sea salt aerosols, volcanic emissions, dust deposition, and emissions from fossil and biomass fuels (Schlesinger and Vengosh 2016). Due to the long distance from the ocean and limited volcanic and human activities, dust deposition is the main component of the atmosphere. Dust deposition in this region is dominated by salt dust storms, primarily consisting of soluble terrestrial salts, gypsum, and borate minerals (Geng et al. 2021; Zhang et al. 2020), which have different B content and isotopic compositions.

The B content and $\delta^{11}B$ average values in halite from the DQSL and XQSL are, respectively, 14.50 mg/kg and 2.1‰ ($n=2$) (Liu et al. 2000), for travertine (calcite, dolomite, and gypsum) are 486.36 mg/kg and − 18.34‰ ($n=4$) (Li and Sun 1996), and for borate minerals (borax and szaibelyite) are − 8.35‰ ($n=3$) (Xiao et al. 1992). If these soluble salts are completely dissolved in atmospheric precipitation, rainwater should have lower $\delta^{11}B$ values. However, the $\delta^{11}B$ value of local rainwater is as high as 16.69‰. The $\delta^{11}B$ average value of mainstream samples (TTRM-1–3), representing the background value of the basin, is 16.15‰ ($n=3$), indicating limited dissolution of salt minerals in rainwater. In addition, the B content in the local rainwater was measured to be 0.04 mg/L, which is significantly higher than the average value in world rivers (0.01 mg/L) (Gaillardet et al. 2014). The previous studies have even reported B content in rainwater in the Da Qaidam area as high as 0.5 mg/L (Xiao et al. 1992), indicating that seasonal salt dust storms in the QB have a significant impact on the B content in atmospheric precipitation and indeed

contribute to the increase in B content in the river water of the basin. However, due to the research area being located in an arid region with very little precipitation, it is evident that atmospheric precipitation cannot be the main source of B in the TTR.

Evaporites are typically composed of rock salt and sulfate minerals (such as gypsum), with B primarily present in fluid inclusions in the rock salt, while sulfate minerals mainly contain B within their crystal lattice. As a result, the B content in evaporites varies greatly, with marine evaporites generally having higher B content than continental (Vengosh et al. 1991). The B content in the rock salt in the DQSL and XQSL is only 0.001% (wt.), and in Qarhan Salt Lake is even lower at 0.0006% (wt.) ($n=43$) (Fan et al. 2015). Although the B content in sulfate minerals in the study area has not been reported, Qin et al. (2018) determined the B content in gypsum from marine evaporite deposits in Laos and found that the average B content in purified gypsum was 0.0004% (wt.) ($n=3$). Rudnev et al. (1985) also confirmed through electron paramagnetic resonance technology that the high boron content (500–3000 ppm) in sedimentary gypsum is caused by boron in the microstructure of boron minerals, detritus, clay minerals, and fluid inclusions, while the boron content in the gypsum mineral structure itself is extremely low (~ 1.0 ppm). In addition, the B content in the travertine (calcite, gypsum, and dolomite) of the DQSL is 0.03% (wt.) (Li and Sun 1996), indicating a generally low B content in the evaporites of the study area. Combining Piper diagrams and the contribution of solute sources, it can be inferred that although solutes in the TTR are primarily derived from the dissolution of evaporites, with chloride salts being the dominant minerals, the contribution of B from the dissolution of evaporites is very limited.

The occurrence state of B in carbonates is primarily determined by the B content and pH of the mother solution during their precipitation period. Generally, marine carbonates have higher B content than terrestrial ones, so the contribution of terrestrial carbonates to riverine B is usually negligible (Chetelat and Gailardet 2005). The Ca/B molar ratio of carbonate rocks can indicate the contribution of boron content from carbonate rock dissolution in rivers. Statistical studies have found that the contribution of boron through this method is consistently less than 5% (Chetelat et al. 2009). Additionally, the exposure of carbonates in the study area is small, and their contribution to the solute of the TTR is also minimal (Figs. 1b and 5). Therefore, the dissolution of carbonates in the study area has a small contribution to B in the TTR.

Silicates typically include igneous rocks, siliceous clastic rocks, and metamorphic rocks (Hartmann and Moosdorf 2012). Among them, granite is the main reservoir of B in igneous rocks, and shale is the main reservoir of B in siliceous clastic rocks (Dürr et al. 2005). However, calculations of the contribution of end-members to the solute of the TTR indicate that the weathering contribution of silicates is very small, only about 0.5%. Therefore, silicates are not the key factor for the high B content in the TTR.

Based on the analysis of B content and $\delta^{11}B$ values in different waters in the study area (Fig. 6), it can be observed that the atmospheric precipitation, tributary TTRT-8, and mainstream TTRM-1–3, which represents the background value of the TTR, exhibit low B content and high $\delta^{11}B$ values, while mainstream samples flowing through Indosinian granite and MVW have high B content and low $\delta^{11}B$ values. Specifically, the average B content of the TTR mainstream (TRM-1–3) is 0.40 mg/L, with an average $\delta^{11}B$ value of 16.15‰ ($n=3$). After passing through the Wulanbaomu and Wubaotu mud volcanoes, the B content of TTRM-4 significantly increases to 2.19 mg/L, about five times higher, while the $\delta^{11}B$ value decreases to 4.71‰. Since the Wulanbaomu and Wubaotu mud volcanoes have perennial outflows of spring water, with B contents of 165.66 mg/L and 77.54 mg/L, respectively (Zhang 2015), and $\delta^{11}B$ values ranging from

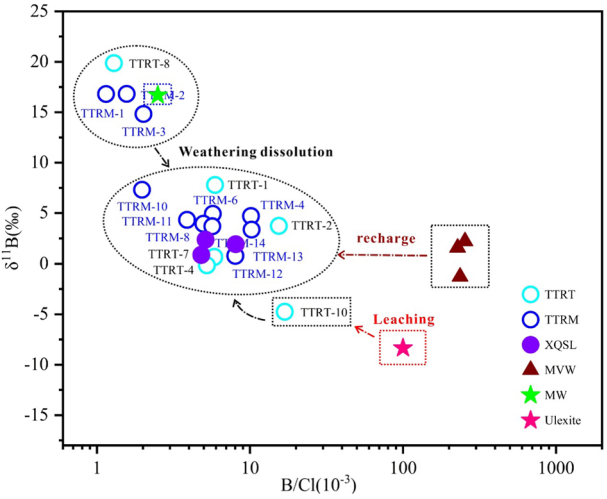

Fig. 6 The B content and $\delta^{11}B$ values of different waters in the study area. The B/Cl value of the ulexite is assumed due to the main component is B with little or no Cl ions in this mineral. TTRT (tributary of the TTR), TTRM (mainstream of the TTR), XQSL (Xiao Qaidam Salt Lake), MW (Meteoric water), and MVW (Mud volcanic water)

−1.26‰ to +2.22‰, the rapid increase in B content and rapid decrease in $\delta^{11}B$ value of the TTRM-4 sample indicate that river water may be influenced by intermittent surface overflow and underground seepage of mud volcano water.

The B content of the main stream TTRM-6 sample in the TTR does not change significantly (1.95 mg/L) after it merges with a tributary flowing through the Juhongtu boron mine. The $\delta^{11}B$ value (4.93‰) also remains low. Although the B content of the TTRT-4 sample in this tributary (1.07 mg/L) is significantly higher than other tributary samples that have not flowed through mud volcanoes or boron mine sites (0.39 mg/L, $n=7$), the $\delta^{11}B$ value of borate minerals deposited in the boron mine site is significantly negative (−8.35‰) (Xiao et al. 1992). It is speculated that the dissolution of borate minerals may not significantly contribute to the B content in the river water during the process of flowing through the Juhongtu boron mine.

The mainstream of the TTR, specifically samples TTRM-5–9, displayed similar TDS and $\delta^{11}B$ values. The average TDS was 756.58 mg/l ($n=5$), with an average $\delta^{11}B$ value of 4.44‰ ($n=2$). In contrast, samples TTRM10-14 showed a significant increase in TDS, with an average of 1223.35 mg/l ($n=5$). The B content gradually increased up to TTRM-14, where it slightly declined due to dilution. However, the overall trend for $\delta^{11}B$ was decreasing, with an average value of 3.90‰ ($n=5$). This is similar to the $\delta^{11}B$ value of HS in the western part of the same tectonic zone (1.34‰, $n=2$), and it can also be compared with the HR (1.90 mg/L, −0.88‰) and the NR (1.36 mg/L, −0.80‰) influenced by hot springs (Zhang et al. 2022). This fully demonstrates the presence of some hot springs or geothermal springs in the granite, which provide a large amount of B to the TTR. Furthermore, it is worth noting that the TTRT-10 from the downstream tributary passing through the granite body shows a trend toward borate dissolution (Fig. 6). This may be due to the presence of deep water circulation in the Indosinian granite body, which leaches boron-bearing minerals in the rock, resulting in a more negative $\delta^{11}B$ value for TTRT-10.

In conclusion, the main sources of boron in the TTR are the mud volcano water in the upper reaches of the river and the possible deep groundwater near the Indosinian granite in the downstream. Atmospheric input and rock mineral weathering leaching contribute less to the boron content (Fig. 7).

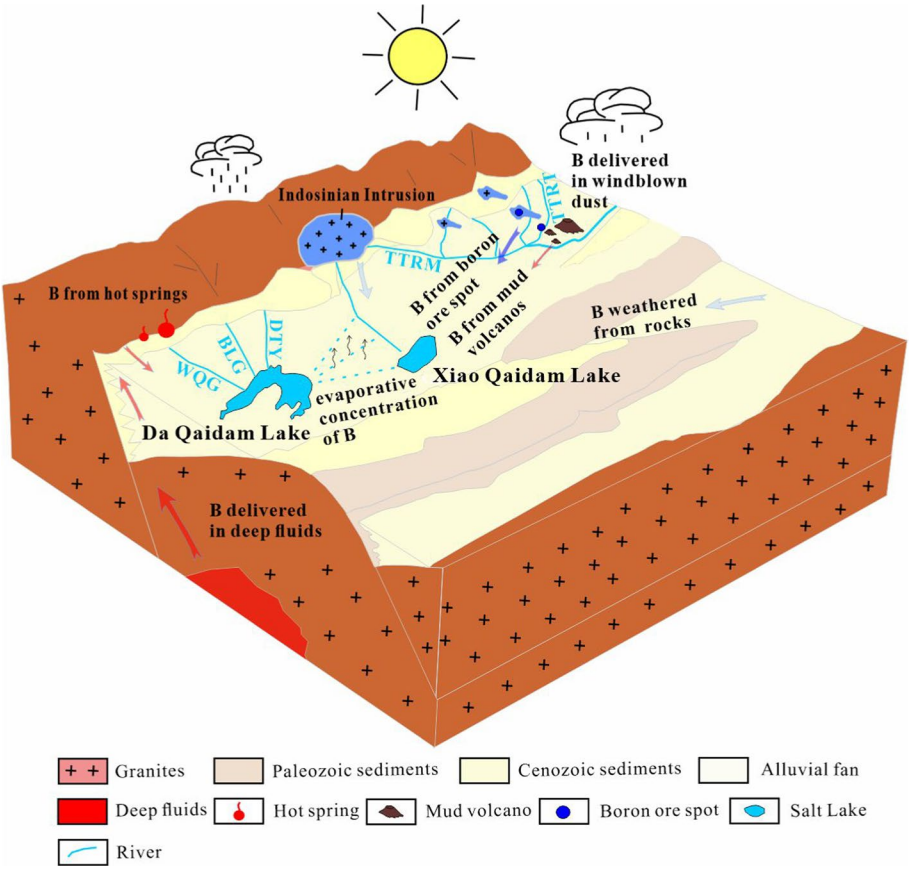

Fig. 7 The conceptual map of the boron deposits formation in the DQSL and XQSL in study area. TTRT (tributary of the TTR), TTRM (mainstream of the TTR), DTY (the river of Datouyang), BLG (the river of Baligou), and WQG (the river of Wenquangou)

5.4 Implication for the Boron Deposit in the Terminal Salt Lake

The diversity of ore-forming materials and ore-forming methods has driven the development of current ore-forming theories. The genetic mechanism of modern salt lake boron deposits is closely related to their geological background and climatic environment, and they are the products of the coupling of tectonics, climate, and provenance. The previous studies have shown that before the Late Pleistocene (> 30 ka BP), the Da and Xiao Qaidam Basins were once a unified freshwater lake basin, and the ancient TTR was an important water source for replenishing the Qaidam ancient lake basin (Yang 1983; Zheng et al. 1989). Until the end of the Late Pleistocene, with the onset of the Late Tali Glaciation, the climate became arid, the water supply decreased sharply, and the uplift of local terrain caused by the influence of new tectonic movements led to the separation of the Da and Xiao Qaidam lakes into their respective evolutionary stages (Zheng et al. 1989). Chronological studies of lacustrine clay deposits beneath the halite layer revealed by drilling cores from the DQSL indicate that the Qaidam ancient lake basin gradually became arid from MIS2 to the Holocene (Madsen et al. 2014). The regional tectonic movements also significantly influenced the evolution of the DQSL and

XQSL basins (Zheng et al. 1989). Sedimentary records show that the first period of salt deposition in the late Pleistocene in the DQSL was located in the western part of the lake, while the second period of salt deposition from the late Pleistocene to the Holocene shifted to the eastern part of the basin.

At the same time, the salt deposition center in the Holocene of the XQSL was also located in the southeastern part of the basin, indicating that the migration of the deposition center was significantly driven by tectonic movements. In addition, the new tectonic movements also influenced the evolution of the ancient TTR. Geophysical data show that there were uplift structures at both ends of the Da Qaidam Lake since the Middle Pleistocene, and the continuous uplift caused the ancient TTR to completely change its course to flow eastward into the Xiao Qaidam Lake at the end of the Late Pleistocene and the beginning of the Holocene (Qaidam Geological Team 1969), which also contributed to the final separation and evolution of the Da and Xiao Qaidam lakes (Zheng et al. 1989).

The TTR is a major B-anomalous surface water system in the northern part of the DQSL and XQSL. The previous studies have suggested that the anomalous B in the TTR is closely related to the development of the NWW fault group in the southern Qilian Mountains upstream of the TTR (Zheng et al. 1989). Although there is a lack of systematic research on the evolution of neotectonic movements in the study area, the geological facts that the Da Qaidam hot springs and the mud volcanoes in the upstream area of the TTR are developed along the NWW fault zone of the southern Qilian Mountains, and the corresponding water types and trace element contents are similar to typical geothermal waters, as well as the good consistency between the ancient calcium carbonate age of the Da Qaidam hot springs (C^{14} age of 24420 ± 1750 a, Yang 1983) and the mineralization age of the Juhongtu boron deposit (OSL age of 0.028 ± 0.002 Ma, Qi et al. 2014), it can be inferred that there may have been a relatively active period of neotectonic movements in the late Pleistocene. This period of tectonic activity drove the formation of the Da Qaidam hot springs and the activity of the mud volcanoes in the upstream area of the TTR, providing abundant source materials for the sedimentary boron deposits in the surrounding depression areas (Wulanbaomu, Kaotiaozhaohuo) and the DQSL.

At the same time, this process also induced the development of small-scale fault structures in the Indosinian granite bodies in the northern part of the DQSL and XQSL, creating conditions for the migration of deep fluids and driving the formation of the Juhongtu ancient hot spring water type boron deposit. In addition, to some extent, this can also explain why the DQSL, which received the abnormally rich soluble boron carried by the ancient TTR during the active tectonic period at the end of the late Pleistocene, ultimately formed significantly higher boron mineral resources than the XQSL (the confirmed B_2O_3 reserves of the XQSL only account for 13% of those of the DQSL, Wei 2002). With the weakening of tectonic activity at the beginning of the Holocene and the diversion of the ancient TTR, the Xiao Qaidam Lake mainly receives the supply of the TTR with significantly reduced boron content (Fig. 7). However, due to the lack of more evidence in sedimentology and related chronology, this understanding still needs further verification through additional work.

6 Conclusions

The TTR is an important source for both the DQSL and XQSL. The water chemistry characteristics of the tributaries and mainstreams of TTR and different solute contributions indicate that the main solute sources in the TTR is the dissolution of evaporite from strata

or surface (evaporation capillary action, salt dust storms, and atmospheric deposition), while the contribution from atmospheric precipitation, carbonates, and silicates weathering is minimal. B content and its isotope compositions suggest that deep groundwater, possibly present in the upstream mud volcanoes and downstream Indosinian granite bodies, are the two main contributors of B in the TTR. The significant difference in resources between the DQSL and XQSL may be attributed to the late Pleistocene period when the DQSL received an exceptionally rich supply of soluble boron carried by the ancient TTR during an active tectonic movement. In contrast, during the early Holocene, due to weakened tectonic activity and the diversion of the ancient TTR, the XQSL mainly received a reduced supply of B from the TTR. These findings are of important for a deeper understanding of the ore-forming mechanism of boron deposits in the DQSL and XQSL, and are helpful to study the origin of salt lake-type boron deposits all around the world.

Supplementary Information The online version contains supplementary material available at https://doi.org/10.1007/s10498-024-09427-6.

Acknowledgements We would like to thank the anonymous reviewers and the editor for their constructive comments and suggestions, which substantially improved the manuscript. This work was supported by the Second Tibetan Plateau Scientific Expedition and Research (STEP) (2019QZKK0805), the Foundation of Qinghai Science & Technology Department (2020-ZJ-734), and the Western Light Foundation of Chinese Academy of Sciences (Grant to Weiliang Miao).

Author Contributions WL helped in sample collection, data analysis, and writing. ZQ helped in sample collection and data analysis. WM helped in disscussion and sample collection. YL and WC helped in sample collection. YD helped in data collection and discussion. BL worked in project design and discussion. XZ worked in project design and revision.

Data Availability No datasets were generated or analysed during the current study.

Declarations

Competing interests The authors declare that they have no known competing financial interests or personal relationships that could have appeared to influence the work reported in this paper.

References

Ali F, Hosmane NS, Zhu YH (2020) Boron chemistry for medical applications. Molecules 25(4):828. https://doi.org/10.3390/molecules25040828

Barth S (1998) Application of boron isotopes for tracing sources of anthropogenic contamination in groundwater. Water Res 32:685–690. https://doi.org/10.1016/S0043-1354(97)00251-0

Cai PJ (2019) Geological and geochemical characteristics of the Kaipinggou ultrabasic complex indications for prospecting in the Northern margin of the Qaidam. Dissertation, China University of Geosciences

Chetelat B, Gaillardet J (2005) Boron isotopes in the Seine River, France: a probe of anthropogenic contamination. Environ Sci Technol 39(8):2486–2493. https://doi.org/10.1021/es048387j

Chetelat B, Liu CQ, Gaillardet J et al (2009) Boron isotopes geochemistry of the Changjiang Basin Rivers. Geochim Cosmochim Acta 73(20):6084–6097. https://doi.org/10.1016/j.gca.2009.07.026

Chhabra R (1996) Soil salinity and water quality. A.A. Balkerna Publishers, Brookfield

China Geological Survey (2004) Geological map of the People's Republic of China 1:2 500000. SinoMaps Press, Beijing

Dang Y (2020) The model of evolution and circulation of groundwater in the Tatalling River Basin, Qaidam Basin. Dissertation, Chang'an University

Dürr HH, Meybeck M, Dürr SH (2005) Lithologic composition of the Earth's continental surfaces derived from a new digital map emphasizing riverine material transfer. Glob Biogeochem Cycles 19(4):1–22. https://doi.org/10.1029/2005GB002515

Dymova MA, Taskaev SY, Richter VA et al (2020) Boron neutron capture therapy: current status and future perspectives. Cancer Commun 40(9):406–421. https://doi.org/10.1002/cac2.12089
Fan QS, Ma YQ, Cheng HD et al (2015) Boron occurrence in halite and boron isotope geochemistry of halite in the Qarhan Salt Lake, western China. Sediment Geol 322:34–42. https://doi.org/10.1016/j.sedgeo.2015.03.012
Foster GL (2008) Seawater pH, pCO2 and [CO2-3] variations in the Caribbean Sea over the last 130 kyr: a boron isotope and B/Ca study of planktic foraminifera. Earth Planet Sci Lett 7:133–140. https://doi.org/10.1016/j.epsl.2008.04.015
Gaillardet J, Dupré B, Louvat P et al (1999) Global silicate weathering and CO2 consumption rates deduced from the chemistry of large rivers. Chem Geol 159(1–4):3–30. https://doi.org/10.1016/S0009-2541(99)00031-5
Gaillardet J, Viers J, Dupré B (2014) Trace elements in river waters. In: Treatise on geochemistry. Elsevier, pp 195–235. https://doi.org/10.1016/B978-0-08-095975-7.00507-6
Galy A, France-Lanord C (1999) Weathering processes in the Ganges-Brahmaputra basin and the riverine alkalinity budget. Chem Geol 159(1–4):31–60. https://doi.org/10.1016/S0009-2541(99)00033-9
Gao C, Yu J, Min X et al (2019) The sedimentary evolution of Da Qaidam Salt Lake in Qaidam Basin, northern Tibetan Plateau: implications for hydro-climate change and the formation of pinnoite deposit. Environ Earth Sci 78:1–15. https://doi.org/10.1007/s12665-019-8480-0
Geng J, Zhang XY, Guo XN et al (2021) Sources of soluble salts in dustfall and their impact on resources and environment in the Qaidam Basin. J Acta Geol Sin 95(07):2082–2098
Qinghai Geological and Mineral Exploration and Development Bureau (QGMB) (1960)
Qinghai Institute of Salt Lakes, Chinese Academy of Sciences (ISLCAS) (1988) The Introduction to Analyzing Methods of Brinesand Salt Deposits, 2nd edition. Science Press, Beijing
Gibbs RJ (1970) Mechanisms controlling world water chemistry. Science 170(3962):1088–2000. https://doi.org/10.1126/science.170.3962.1088
Grew ES (2015) Boron-the crustal element. Elements 11(3):162–163
Han JB, Xu JX, Hussain SA et al (2021) Origin of boron in the gas Hure Salt Lake of Northwestern Qaidam Basin, China: evidence from hydrochemistry and boron isotopes. Acta Geol Sin-Engl Ed 95:531–540. https://doi.org/10.1111/1755-6724.14377
Hartmann J, Moosdorf N (2012) The new global lithological map database GLiM: a representation of rock properties at the earth surface. Geochem Geophys Geosystems 13(12):2012GC004370. https://doi.org/10.1029/2012GC004370
Jiang SY (2001) Boron isotope geochemistry of hydrothermal ore deposits in China: a preliminary study. Phys Chem Earth 26:851–858. https://doi.org/10.1016/S1464-1895(01)00132-6
Jiang SY, Yu JM, Lu JJ (2004) Trace and rare-earth element geochemistry in tourmaline and cassiterite from the Yunlong tin deposit, Yunnan, China: implication for migmatitic-hydrothermal fluid evolution and ore genesis. Chem Geol 209:193–213. https://doi.org/10.1016/j.chemgeo.2004.04.021
Jiang SY, Radvanec M, Nakamura E et al (2008) Chemical and boron isotopic variations of tourmaline in the Hnilec granite-related hydrothermal system, Slovakia: constraints on magmatic and metamorphic fluid evolution. Lithos 106:1–11. https://doi.org/10.1016/j.lithos.2008.04.004
Jiang PW, Fan QS, Qin ZJ et al (2021) The distribution characteristics of boron in water-surrounding rocks in Qaidam Basin and discussion on the source of its enrichment area. J Salt Lake Res 29(01):44–55
Kakihana H, Kotaka M, Satoh S et al (1977) Fundamental studies on the ion-exchange separation of boron isotopes. B Chem Soc Jpn 50(1):158–163. https://doi.org/10.1246/bcsj.50.158
Kong FC, Yang YK, Luo X et al (2021) Deep hydrothermal and shallow groundwater borne lithium and boron loadings to a mega brine lake in Qinghai Tibet Plateau based on multi-tracer models. J Hydrol 598:126313. https://doi.org/10.1016/j.jhydrol.2021.126313
Li JZ, Sun DP (1996) Research on boron isotope geochemistry of Da Qaidam Salt Lake. Geochimica 3:277–285
Li QK, Wang JP, Wu C et al (2021) Hydrochemistry and Sr-S isotope constraints on the source of lithium in the Nalenggele river and its terminal lakes, Qaidam Basin. Acta Geol Sin 95(7):2169–2182
Li BK (2022) Material source, migration process and formation model of boron-rich salt lake in Qinghai-Tibet Plateau, Qinghai Institute of Salt Lakes, Chinese Academy of Sciences
Lin YJ, Zheng MP, Liu XF (2017) Boron resource of salt lakes in Qinghai-Tibet Plateau. Sci Technol Rev 35(12):77–82
Liu WG, Xiao YK, Peng ZC et al (2000) Boron concentration and isotopic composition of halite from experiments and salt lakes in the Qaidam Basin. Geochim Cosmochim Acta 64(13):2177–2183. https://doi.org/10.1016/S0016-7037(00)00363-X

López Steinmetz RL (2017) Lithium- and boron-bearing brines in the central andes: exploring hydrofacies on the eastern Puna Plateau between 23° and 23°30′S. Miner Depos 52(1):35–50. https://doi.org/10.1007/s00126-016-0656-x

Lü YY, Zheng M, Chen W et al (2014) Origin of boron in the damxung Co Salt Lake (Central Tibet): evidence from boron geochemistry and isotopes. Acta Geol Sin (engl Ed) 47(5):513–523. https://doi.org/10.2343/geochemj.2.0273

Madsen DB, Lai ZP, Sun YJ et al (2014) Late Quaternary Qaidam lake histories and implications for an MIS 3 "Greatest Lakes" period in northwest China. J Paleolimnol 51:161–177. https://doi.org/10.1007/s10933-012-9662-x

Mao HR, Liu CQ, Zhao ZQ (2019) Source and evolution of dissolved boron in rivers: insights from boron isotope signatures of end-members and model of boron isotopes during weathering processes. Earth Sci Rev 190:439–459. https://doi.org/10.1016/j.earscirev.2019.01.016

Miao WL, Zhang XY, Li YL et al (2022) Lithium and strontium isotopic systematics in the Nalenggele River catchment of Qaidam basin, China: quantifying contributions to lithium brines and deciphering lithium behavior in hydrological processes. J Hydrol 614:128630. https://doi.org/10.1016/j.jhydrol.2022.128630

Moon S, Huh Y, Qin J et al (2007) Chemical weathering in the Hong (Red) River Basin: rates of silicate weathering and their controlling factors. Geochim Cosmochim Acta 71(6):1411–1430. https://doi.org/10.1016/j.gca.2006.12.004

Muttik N, Kirsimae K, Newsom HE et al (2011) Boron isotope composition of secondary smectite in suevites at the Ries crater, Germany: boron fractionation in weathering and hydrothermal processes. Earth Planet Sci Lett 310:244–251. https://doi.org/10.1016/j.epsl.2011.08.028

Noh H, Huh Y, Qin J et al (2009) Chemical weathering in the three rivers region of eastern Tibet. Geochim Cosmochim Acta 73(7):1857–1877. https://doi.org/10.1016/j.gca.2009.01.005

Pang W, He WG, Yuan DY et al (2015) The Paleoseismic characteristics of the Qinghai Da Qaidam Fault. Earth Sci Environ 37(3):87–103

Pennisi M, Leeman WP, Tonarini S et al (2000) Boron, Sr, O, and H isotope geochemistry of groundwaters from Mt. Etna (Sicily)-hydrologic implications. Geochem Cosmochim Acta 64:961–974. https://doi.org/10.1016/S0016-7037(99)00382-8

Piper AM (1944) A graphic procedure in the geochemical interpretation of water-analyses. EOS Trans Am Geophys Union 25(6):914–928

Qaidam Geological Team (1969) Final geological exploration report of Da Qaidam Lake boron deposit

Qi LJ, Zheng MP, Wu GP et al (2014) Characteristics and forming process of Juhongtu boron deposit in Yashatu, Qinghai Province. Sci Technol Rev 32(35):50–60

Qin ZJ, Zhang XR, Peng ZK et al (2018) Extraction and separation of boron in anhydrite and gypsum minerals and its isotopic measurement by thermal ionization mass spectrometry. Chin J Anal Chem 46:48–54

Qu B, Zhang Y, Kang S et al (2019) Water quality in the Tibetan Plateau: major ions and trace elements in rivers of the "Water Tower of Asia." Sci Total Environ 649:571–581. https://doi.org/10.1016/j.scitotenv.2018.08.316

Rose EF, Chaussidon M, France-Lanord C (2000) Fractionation of boron isotopes during erosion processes: the example of Himalayan rivers. Geochem Cosmochim Acta 64:397–408. https://doi.org/10.1016/S0016-7037(99)00117-9

Rudnev V, Rakov LT, Malinko SV (1985) Boron in the structures of calcite and anhydrite: an indicator of mineralization? Int Geol Rev 27(2):223–229. https://doi.org/10.1080/00206818509466409

Schlesinger WH, Vengosh A (2016) Global boron cycle in the Anthropocene. Glob Biogeochem Cycles 30(2):219–230. https://doi.org/10.1002/2015GB005266

Song S, Niu Y, Su L et al (2013) Tectonics of the North Qilian Orogen, NW China. Gondwana Res 23(4):1378–1401. https://doi.org/10.1016/j.gr.2012.02.004

Stober I, Zhong J, Zhang L et al (2016) Deep hydrothermal fluid–rock interaction: the thermal springs of Da Qaidam, China. Geofluids 16(4):711–728. https://doi.org/10.1111/gfl.12190

Sun DP, Wang YH, Qi HP et al (1989) A preliminary investigation on boron isotopes in Da Qaidam and Xiao Qaidam saline lakes of Qaidam Basin, China. Chin Sci Bull 38:320–324

Vengosh A, Chivas AR, McCulloch MT et al (1991) Boron isotope geochemistry of Australian salt lakes. Geochem Cosmochim Acta 55:2591–2606. https://doi.org/10.1016/0016-7037(91)90375-F

Vengosh A, Chivas AR, Starinsky A et al (1995) Chemical and boron isotope compositions of nonmarine brines from the Qaidam Basin, Qinghai, China. Chem Geol 120(1–2):135–154. https://doi.org/10.1016/0009-2541(94)00118-R

Vengosh A, De Lange GJ, Starinsky A (1998) Boron isotope and geochemical evidence for the origin of Urania and Bannock brines at the eastern Mediterranean: effect of water-rock interactions. Geochem Cosmochim Acta 62:3221–3228. https://doi.org/10.1016/S0016-7037(98)00236-1

Wang SM, Xue B (1998) The relationship between regional environmental differentiation in China and the Asian monsoon revealed by lake records since the Middle Pleistocene. Acta Geol Sin (engl Ed) 3:288. https://doi.org/10.19762/j.cnki.dizhixuebao.1998.03.018

Wei XJ (2002) General situation and development prospect of potassium boron in salt lake in Qaidam Basin. Manag Strategy Qinghai Land Resour 2002(Suppl):64–69

Wei HZ, Jiang SY, Tan HB et al (2014) Boron isotope geochemistry of salt sediments from the Dongtai salt lake in Qaidam Basin: boron budget and sources. Chem Geol 380:74–83. https://doi.org/10.1016/j.chemgeo.2014.04.026

Williams LB, Hervig RL (2004) Boron isotope composition of coals: a potential tracer of organic contaminated fluids. Appl Geochem 19(10):1625–1636. https://doi.org/10.1016/j.apgeochem.2004.02.007

Wu W (2016) Hydrochemistry of Inland Rivers in the north Tibetan Plateau: constraints and weathering rate estimation. Sci Total Environ 541:468–482. https://doi.org/10.1016/j.scitotenv.2015.09.056

Wu LL, Huh Y, Qin JH et al (2005) Chemical weathering in the upper Huang He (Yellow River) draining the eastern Qinghai–Tibet plateau. Geochim Cosmochim Acta 69(22):5279–5294. https://doi.org/10.1016/j.gca.2005.07.001

Wu W, Xu S, Yang J et al (2008) Silicate weathering and CO_2 consumption deduced from the seven Chinese rivers originating in the Qinghai–Tibet Plateau. Chem Geol 249(3–4):307–320. https://doi.org/10.1016/j.chemgeo.2008.01.025

Xiao YK, Beary ES, Fassett JD (1988) An improved method for the high-precision isotopic measurement of boron by thermal ionization mass spectrometry. Int J Mass Spectrom Ion Process 85(2):203–213. https://doi.org/10.1016/0168-1176(88)83016-7

Xiao YK, Sun DP, Wang YH et al (1992) Boron isotopic compositions of brine, sediments, and source water in Da Qaidam Lake, Qinghai, China. Geochim Cosmochim Acta 56(4):1561–1568. https://doi.org/10.1016/0016-7037(92)90225-8

Xiao YK, Qi HP, Wang YH (1994) Lithium isotopic compositions of brine, sediments and source water in DaQaidam Lake, Qinghai, China. Geochemistry. https://doi.org/10.19700/j.0379-1726.1994.04.003

Xiao YK, Shirdkar P, Liu WG et al (1999) Research on boron isotope geochemistry of salt lakes in the Qaidam Basin, Qinghai Province. Prog Nat Sci 7:38–44

Xiao YK, Swihart GH, Xiao Y (2001) A preliminary experimental study of the boron concentration in vapor and the isotopic fractionation of boron between seawater and vapor during evaporation of seawater. Sci China Ser B 44:540–551. https://doi.org/10.1007/BF02880685

Xiao J, Xiao YK, Jin ZD et al (2013) Boron isotope variations and its geochemical application in nature. Aust J Earth Sci 60(4):431–447. https://doi.org/10.1080/08120099.2013.813585

Yang Q (1983) Geological overview of the large and small Qaidam salt lake boron deposits in the Qaidam Basin, Qinghai Province. Qinghai Geol 3:38–63

Zhang PX (1987) Salt lake in Qaidam Basin. Science Press, Beijing

Zhang SH (2005) Environmental quality assessment of groundwater in Qaidam Basin. Environ Qinghai 04:162–165

Zhang XF (2014) Mineralogy and genesis study of boron mineralization points in the Ju laterite and surrounding mud volcanoes in the Yashatu area. Chinese Academy of Geological Sciences

Zhang XY, Li WX, Geng J et al (2020) Salt dust storms ang their impacts on resources and ecological environment in Qaidam Basin. J Salt Lake Res 28(1):11–17

Zhang Y, Tan HB, Cong PX et al (2022) Boron and lithium isotopic constraints on their origin, evolution, and enrichment processes in a river-groundwater-salt lake system in the Qaidam Basin, northeastern Tibetan Plateau. Ore Geol Rev 149:105110. https://doi.org/10.1016/j.oregeorev.2022.105110

Zhao JC, Li WP, Peng JH (2007) Origin and environmental significance of major elements and Sr isotope ratios in rivers originating from Tanggula Mountains. Mod Geol 21(04):591–599

Zheng MP, Xiang J, Wei XJ et al (1989) Salinelake on the Qing-hai-Xizang (Tibet) Plateau. Science Press, Beijing

Zheng X, Nel W, Peng JC et al (2023) Hydrochemistry, chemical weathering and their significance on carbon cycle in the Heilong (Amur) River Basin, Northeast China. Chemosphere 327:138542. https://doi.org/10.1016/j.chemosphere.2023.138542

Zhu YZ, Li ZY, Wu BH et al (1990) The formation of the Qarhan Saline Lakes as viewed from the neotectonic movement. Acta Geol Sin 1:13–21

Zhu GF, Su YH, Feng Q (2008) The hydrochemical characteristics and evolution of groundwater and surface water in the Heihe River Basin, Northwest China. Hydrogeol J 16(1):167–182. https://doi.org/10.1007/s10040-007-0216-7